Influence of WFIKKN1 on BMP1-mediated activation of latent myostatin

György Szláma, Viktor Vásárhelyi, Mária Trexler and László Patthy

Institute of Enzymology, Research Centre for Natural Sciences, Hungarian Academy of Sciences, Budapest, Hungary

The NTR domain of WFIKKN1 protein has been shown to have significant affinity for the prodomain regions of promyostatin and latent myostatin but the biological significance of these interactions remained unclear. In view of its role as a myostatin antagonist, we tested the assumption that WFIKKN1 inhibits the release of myostatin from promyostatin and/or latent myostatin. WFIKKN1 was found to have no effect on processing of promyostatin by furin, the rate of cleavage of latent myostatin by BMP1, however, was significantly enhanced in the presence of WFIKKN1 and this enhancer activity was superstimulated by heparin. Unexpectedly, WFIKKN1 was also cleaved by BMP1 and our studies have shown that the KKN1 fragment generated by BMP1-cleavage of WFIKKN1 contributes most significantly to the observed enhancer activity. Analysis of a pro-TGF-β -based homology model of homodimeric latent myostatin revealed that the BMP1-cleavage sites are buried and not readily accessible to BMP1. In view of this observation, the most plausible explanation for the BMP1-enhancer activity of the KKN1 fragment is that it shifts a conformational equilibrium of latent myostatin from the closed circular structure of the homodimer to a more open form, making the cleavage sites more accessible to BMP1. On the other hand, the observation that the enhancer activity of KKN1 is superstimulated in the presence of heparin is explained by the fact KKN1, latent myostatin, and BMP1 have affinity for heparin and these interactions with heparin increase the local concentrations of the reactants thereby facilitating the action of BMP1.

Introduction

Myostatin is a negative regulator of skeletal muscle growth: mice lacking myostatin are characterized by a significant increase in skeletal muscle mass [1]. Mutations of the myostatin gene that interfere with the formation of mature myostatin were also shown to cause hypermuscularity in mice, cattle, dog, and human [2–7]. In addition to its role in muscle development, myostatin is also involved in regulation of

adipose tissue: in Mstn−/− mice, adipose tissue size is significantly reduced [8,9].

Myostatin is synthesized as an inactive precursor protein, containing an N-terminal prodomain and a C-terminal growth factor domain [10]. In promyostatin, two molecules are linked through a single disulfide bond present in the C-terminal growth factor domain. Active myostatin (corresponding to the covalently linked, homodimeric growth factor domain) is released from promyostatin by proteolytic processing. First, furin-type proprotein convertases cleave both chains of the precursor at the boundary of the N-terminal prodomain and the C-terminal growth factor domain. The importance of this step in the control of myostatin activity is underlined by the observation that the common K153R polymorphism of human promyostatin that significantly increases the rate of its proteolysis by furin is associated with obesity and lower muscle strength [11]. Furin-cleavage of promyostatin, however, does not lead to the release of active myostatin: the myostatin prodomains and the disulfide-bonded growth factor domains remain associated, forming a noncovalent myostatin/prodomain complex [12]. As the myostatin/prodomain complex does not bind to the myostatin receptor, Act RIIB, the noncovalent myostatin/prodomain complex is referred to as latent myostatin [12,13].

Active myostatin is released from latent myostatin by proteases of the BMP1/Tolloid family that cleave the prodomain of myostatin, thereby disrupting the noncovalent myostatin/prodomain complex [14]. The key importance of BMP1-mediated cleavage of latent myostatin for the release of mature myostatin is supported by the observation that mice carrying a mutation that renders the myostatin prodomain BMP1-resistant exhibit significant increase in muscle mass [15].

Several myostatin antagonists exist that may control the activity of mature myostatin. Lee and McPherron were the first to show that follistatin, an activin antagonist, is also a potent inhibitor of myostatin [12]. Furthermore, Hill *et al.* [16] have shown that myostatin is bound to another inhibitory binding protein, the FSTL3/FLRG protein (the product of the follistatin-related gene, FLRG).

Two other follistatin-related proteins, the products of the *WFIKKN1* and *WFIKKN2* genes were also shown to have high affinity for myostatin [17,18]. Significantly, WFIKKN1 and WFIKKN2 have higher specificity for myostatin (and the closely related GDF-11) than follistatin or FLST3/FLRG protein [19]. The physiological significance of WFIKKN2 protein as a key regulator of myostatin activity is supported by the

observation that delivery of *WFIKKN2* gene into the muscles of mice resulted in an approximately 30% increase in muscle mass and that transgenic mice over-expressing WFIKKN2 protein have larger muscles compared to wild-type animals [20,21].

WFIKKN1 and WFIKKN2 are closely related proteins that, in addition to a follistatin domain, contain WAP domain, an immunoglobulin domain, two Kunitz domains, and an NTR domain [22,23]. The names of these proteins refer to the linear sequence of their constituent WAP, follistatin, immunoglobulin, Kunitz, Kunitz, and NTR domains [22,23]. In Fig. 1, we show a schematic representation of the domain architecture of the WFIKKN1 protein.

Our studies on these WFIKKN proteins have revealed that their follistatin domains are primarily responsible for the myostatin antagonist activity [18,19,24], but relatively little is known about the function of the other domain types.

As WAP, Kunitz, and NTR domains have been implicated in inhibition of various types of proteases, we have hypothesized that the corresponding domains of WFIKKN proteins might also function as protease inhibitors [22–24]. Full-length WFIKKN proteins were found to inhibit the proteolytic activity of bovine trypsin but they had no effect on the peptidolytic activities of bovine elastase, chymotrypsin, tissue-type plasminogen activator, urokinase-type plasminogen activator, furin, and BMP1 [24]. At the domain level, the trypsin inhibitory activity of WFIKKN proteins was assigned to their second Kunitz-type domain [25].

Interestingly, the NTR domain of WFIKKN1 (but not of WFIKKN2) was found to have significant affinity for myostatin prodomain [18,26]. This difference between WFIKKN1 and WFIKKN2 is also reflected in their interactions with promyostatin and latent myostatin; although WFIKKN1 has affinity for both promyostatin and latent myostatin, WFIKKN2 had no affinity for these proteins, suggesting that the NTR/prodomain interaction mediates the interaction of WFIKKN1 with promyostatin and latent myostatin [18,26]. Detailed analysis of the WFIKKN1–prodomain interaction revealed that WFIKKN1 binds the C-terminal subdomain of myostatin prodomain, but not the N-terminal subdomain that plays a critical role in the interaction of the prodomain with mature myostatin [26]. It thus appears that myostatin prodomain consists of two functionally distinct subdomains: the N-terminal subdomain binds mature myostatin, whereas the C-terminal subdomain binds WFIKKN1.

Very little is known about the biological significance of the interaction of WFIKKN1 with myostatin propeptide, promyostatin, and latent myostatin. In
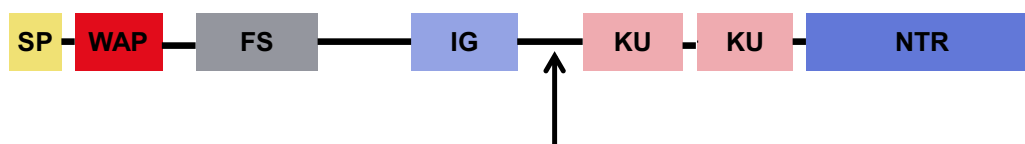
Fig. 1. Domain architecture of WFIKKN1 protein. The name of this protein is an acronym that refers to its constituent WAP-, follistatin-, immunoglobulin-, Kunitz-type protease inhibitory domains and NTR domain. The arrow indicates the position of the peptide bond that is cleaved by BMP1.

view of the role of WFIKKN1 and WFIKKN2 as myostatin antagonists, we have speculated that the interaction of WFIKKN1 with promyostatin and latent myostatin might also serve as an antimyostatic function, e.g., it may interfere with the release of mature growth factor from promyostatin and/or latent myostatin [24].

The goal of our present work was to investigate the assumption that the interaction of WFIKKN1 with the myostatin prodomain might inhibit furin-cleavage of promyostatin and/or BMP1-cleavage of latent myostatin.

Our studies have shown that WFIKKN1 has no influence on the rate of furin-mediated cleavage of promyostatin. The rate of cleavage of latent myostatin by BMP1, however, was significantly enhanced in the presence of WFIKKN1 and this enhancer activity was superstimulated by heparin. Unexpectedly, when latent myostatin was incubated with BMP1 in the presence of WFIKKN1—concomitant with the cleavage of latent myostatin—WFIKKN1 was also cleaved by BMP1 (Fig. 1). Our studies have shown that the KKN1 fragment generated by BMP1-cleavage of WFIKKN1 protein contributes most significantly to the observed enhancer activity. Cleavages of latent myostatin and WFIKKN1 protein by BMP1 are thus synergistic in the sense that they promote the liberation of active myostatin from latent myostatin.

Results and Discussion

Rate of cleavage of promyostatin by furin is not affected by the promyostatin–WFIKKN1 interaction

Promyostatin was digested with furin in the presence and absence of WFIKKN1 and WFIKKN2 proteins, samples were withdrawn at various time points, and their composition was analyzed by SDS/PAGE as described in Materials and methods. As shown in Fig. 2, neither WFIKKN1 nor WFIKKN2 had any influence on the rate of decrease in the amount of

intact promyostatin and increase in the amount of myostatin prodomain.

As in these experiments, we employed a molar excess of WFIKKN1 over promyostatin, and the concentration of WFIKKN1 exceeded the K_d value of the WFIKKN1/promyostatin interaction [26]. The lack of WFIKKN1's influence on the rate of furin-cleavage suggests that the accessibility of the furin-cleavage site of the myostatin precursor is not impaired in the WFIKKN1/promyostatin complex. In other words, the interaction of the NTR domain of WFIKKN1 with the prodomain of promyostatin does not shield the furin-cleavage site of the precursor.

Rate of cleavage of latent myostatin by BMP1 is significantly enhanced in the presence of WFIKKN1 concomitant with cleavage of WFIKKN1

Latent myostatin was digested with BMP1 in the absence and presence of increasing concentrations (0.5–4 μM) of WFIKKN1 protein and the samples were analyzed by SDS/PAGE as described in Materials and methods. As shown in Fig. 3, the rate of cleavage of myostatin prodomain by BMP1 was significantly enhanced in the presence of WFIKKN1 (Fig. 3, panel B), and this rate enhancement was much more pronounced when heparin was also included in the reaction mixture (Fig. 3, panel C). Half-maximal enhancer activity was achieved by ~ 0.5 μM of WFIKKN1 in the absence of heparin and by ~ 1 μM of WFIKKN1 in the presence of heparin.

Surprisingly, concomitant with the cleavage of myostatin prodomain, WFIKKN1 was also cleaved by BMP1: as a result of cleavage of WFIKKN1 (Mr ~ 60 kDa) by BMP1 a diffuse band with an apparent Mr of ~ 30 kDa appeared (Fig. 3, last two lanes in panel A). Quantitative evaluation of the gels has shown that the rate of cleavage of WFIKKN1 by BMP1 is slightly, but significantly ($P < 0.01$, Student's *t*-test) enhanced in the presence of heparin.

These data indicate that the interaction of the NTR domain of WFIKKN1 with the prodomain of latent
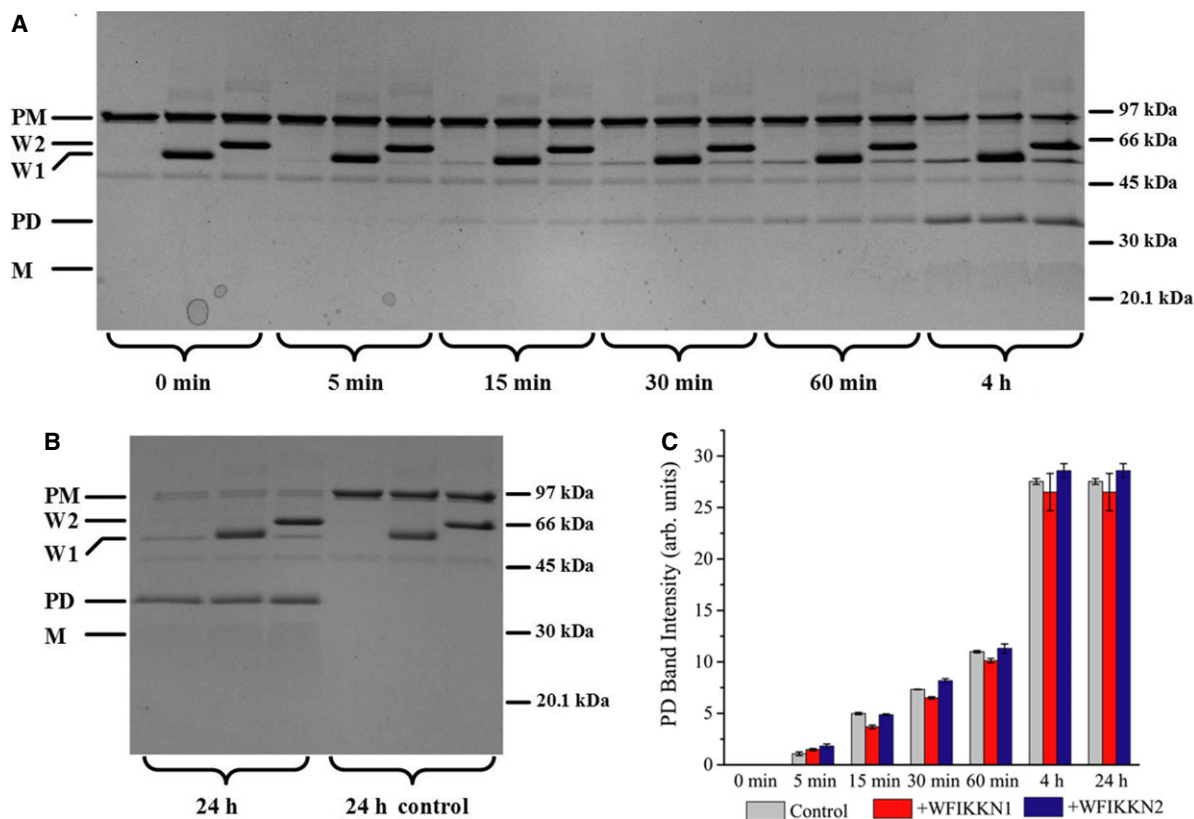
Fig. 2. Furin-cleavage of promyostatin is not affected by the presence of WFIKKN1 or WFIKKN2. Promyostatin (500 nM) was incubated with recombinant human furin (1 µg·mL^{-1}) in 100 mM TRIS/HCl, 150 mM NaCl, 1 mM CaCl2, 100 mM phenylmethanesulphonylfluoride buffer, pH 8.0 at 28 °C for 0 min, 5 min, 15 min, 30 min, 1 h, 4 h (panel A), and 24 h (panel B) in the presence or absence of WFIKKN1 (1.5 µM) or WFIKKN2 (1.5 µM) and nonreduced samples were analyzed by SDS/PAGE analysis; the gels were stained with Coomassie Brilliant Blue G-250. At each time-point, lane 1 shows control samples lacking WFIKKN1 or WFIKKN2, lane 2 shows samples containing WFIKKN1, and lane 3 shows samples containing WFIKKN2. Panel B also shows the results of control experiments, indicating that in the absence of furin, no cleavage of promyostatin occurred. Panel C shows the quantitative evaluation of the data, indicating that neither WFIKKN1 nor WFIKKN2 had any influence on the rate of increase in the amount myostatin prodomain (the error bars indicate the standard error of the mean, *n* = 3). Abbreviations: M, myostatin; PD, myostatin prodomain; PM, promyostatin; W1, WFIKKN1; W2, WFIKKN2.

myostatin [18,26] increases the susceptibility of the prodomain to BMP1-cleavage but it is not clear whether the enhancer activity is mediated by the NTR domain of full-length WFIKKN1 or of the WFIKKN fragment(s) generated by BMP1-cleavage.

BMP1 cleaves the Arg287–Asp288 bond of WFIKKN1

To characterize the BMP1-cleavage site of WFIKKN1, we have incubated the protein (25 µg) with 2.5 µg BMP1 in 100 µL of buffer containing 25 mM Tris/HCl, 150 mM NaCl, 5 mM CaCl$_2$, 1 µM ZnCl$_2$, pH 7.5 at 37 °C for 6 h. Addition of BMP1 (2.5 µg) was repeated and digestion was continued for a total of 16 h, then the C-terminal fragment carrying the C-terminal His-tag of the WFIKKN1 protein [18] was

isolated by affinity chromatography on a 50 µL Ni-NTA Sepharose column and by SDS/PAGE. N-terminal sequence analysis of the ~ 30 kDa C-terminal fragment yielded the amino acid sequence DAAPSI-PAPAEXLPDV corresponding to residues 288–303 of human WFIKKN1 indicating that the fragment was generated by cleavage of the Arg287–Asp288 peptide bond.

Residues Arg287–Asp288 are located between the immunoglobulin and the first Kunitz domains of WFIKKN1 (Fig. 1), thus cleavage of this peptide bond by BMP1 generates WFI1 and KKN1 fragments (calculated molecular masses: 28 845 and 29 181 Da, respectively) corresponding to the N-terminal and a C-terminal halves of the protein.

The observation that BMP1 cleaves the N-terminal peptide bond of an aspartic residue of WFIKKN1 is
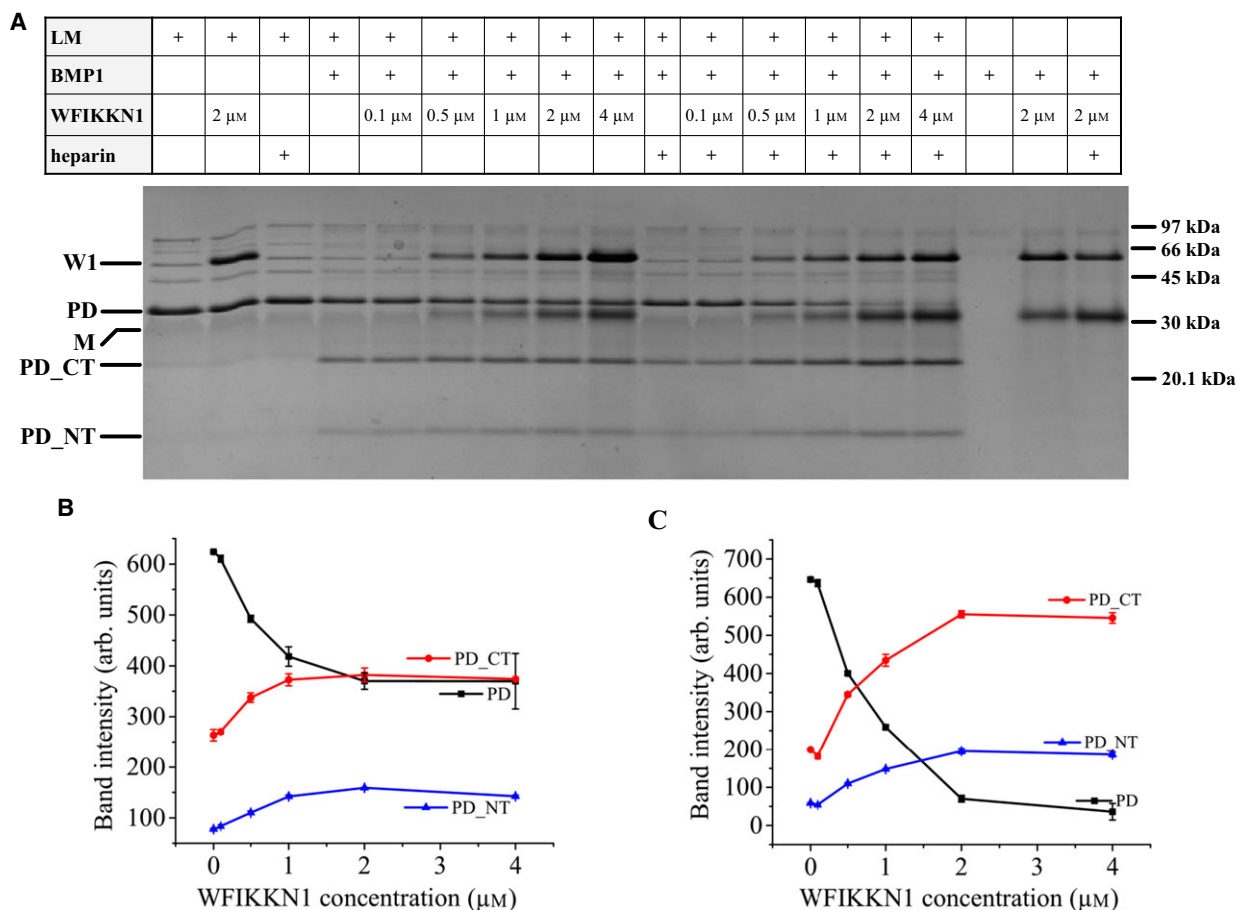
A

LM	+	+	+	+	+	+	+	+	+	+	+	+	+	+	+			
BMP1				+	+	+	+	+	+	+	+	+	+	+	+	+	+	+
WFIKKN1		2 μM			0.1 μM	0.5 μM	1 μM	2 μM	4 μM		0.1 μM	0.5 μM	1 μM	2 μM	4 μM		2 μM	2 μM
heparin			+							+	+	+	+	+	+			+

Fig. 3. Rate of cleavage of latent myostatin by BMP1 is significantly enhanced in the presence of WFIKKN1 concomitant with cleavage of WFIKKN1. Latent human myostatin (LM, 500 nM) was digested with 50 nM BMP1 in 25 mM HEPES buffer, pH 7.5 containing 150 mM NaCl, 5 mM CaCl$_2$, 1 mM ZnCl$_2$, and 1 mM furin inhibitor I at 37 °C for 16 h in the presence of increasing concentrations of WFIKKN1, in the absence or presence of heparin (5 μg·mL^{-1}). WFIKKN1 was also digested with BMP1 in the absence of latent myostatin in the presence or absence heparin. Nonreduced samples were analyzed by SDS/PAGE analysis; the gels were stained with Coomassie Brilliant Blue G-250 (panel A). Panels B and C show the progress of BMP1 cleavage of prodomains as assessed from the decrease of the amount of uncleaved prodomain (PD) and increase in the amount of C-terminal (PD_CT) and N-terminal (PD_NT) fragments resulting from BMP1-cleavage of the prodomain; the error bars indicate the standard error of the mean, *n* = 3. Note that the amounts of PD_NT and PD_CT are significantly higher in the presence of 0.5–4 μM WFIKKN1 than in its absence (panel B). Also note that in the presence of heparin and 2–4 μM WFIKKN1, cleavage of myostatin prodomain (PD) is practically complete, whereas in the absence of WFIKKN1, the majority of PD is still intact (panel C). Note that heparin also increases the rate of cleavage of WFIKKN1 (see last two lanes in panel A). Abbreviations: LM, latent myostatin; M, myostatin; PD, myostatin prodomain; PD_CT, C-terminal fragment of myostatin prodomain; PD_NT, N-terminal fragment of myosatin prodomain; W1, WFIKKN1.

in harmony with the strict preference of BMP1 for Asp residues in the P1′ position. In the crystal structure of BMP1, there is an arginine (Arg176) in the S1′ pocket; the presence of this basic residue in S1′ fits well with the known specificity of BMP1 for an aspartic acid in the P1′ position [27].

The importance of Asp288 of WFIKKN1 for its susceptibility to BMP1-cleavage is supported by the fact that its substitution by alanine rendered the protein resistant to cleavage by BMP1 (Fig. 4, last two

lanes in panel A). Aside from its Asp specificity at the P1′ position, BMP1 has little preference for residues at positions adjoining the cleavage sites of protein substrates (Table 1 and fig. 4 in [28]), suggesting that accessibility of Xaa-Asp bonds plays an important role in determining whether they serve as BMP1-cleavage sites [28].

It is noteworthy in this respect that the BMP1-cleavage site at Arg287–Asp288 of WFIKKN1 is in a flexible low-complexity region (residues 274–298,
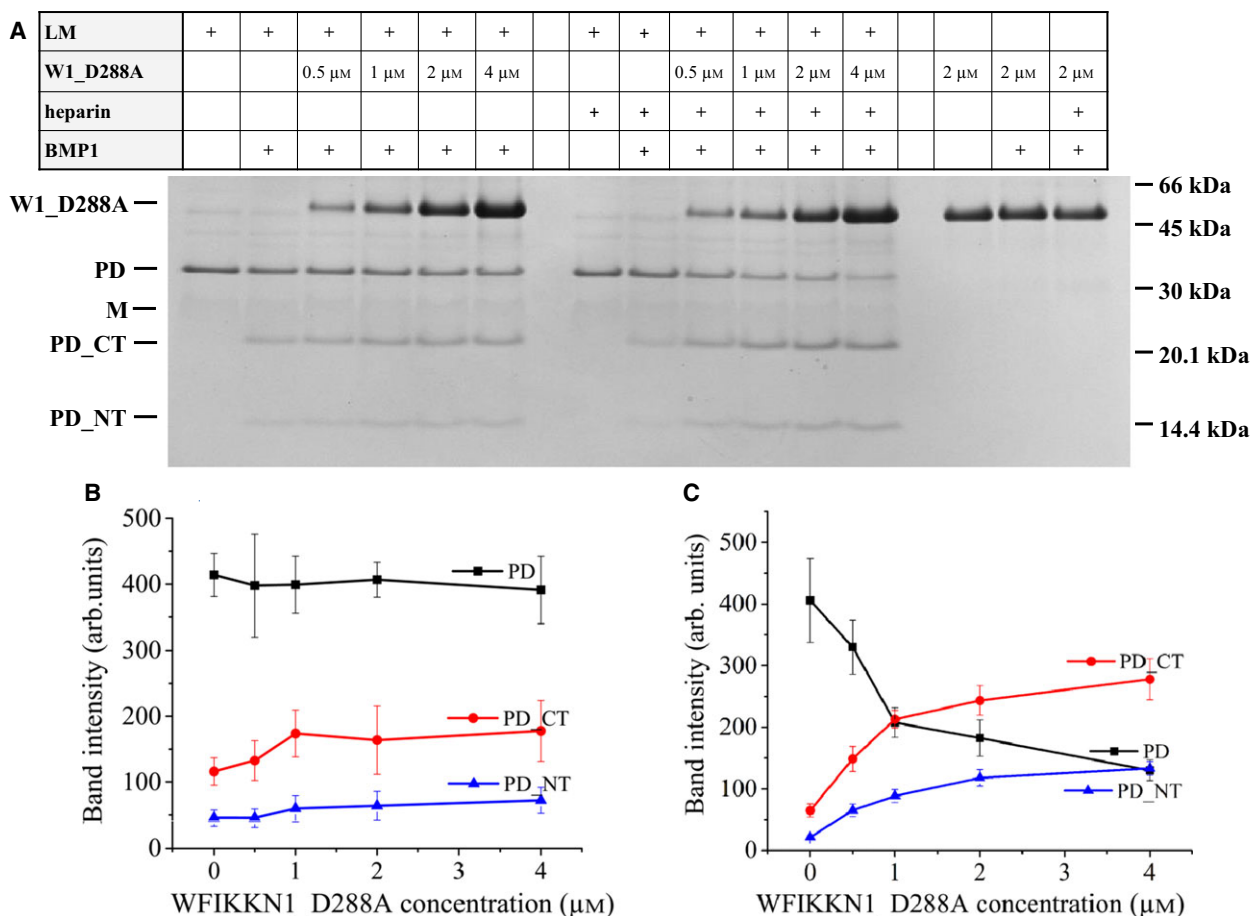
Fig. 4. Rate of cleavage of latent myostatin by BMP1 is not enhanced by the D288A mutant WFIKKN1 in the absence of heparin. Latent human myostatin (LM, 500 nM) was digested with 50 nM BMP1 in 25 mM HEPES buffer, pH 7.5 containing 150 mM NaCl, 5 mM CaCl2, 1 mM ZnCl$_2$, and 1 mM furin inhibitor I at 37 °C for 16 h in the presence of increasing concentrations of the D288A mutant WFIKKN1, in the absence or presence of heparin (5 µg·mL^{-1}). Nonreduced samples were analyzed by SDS/PAGE analysis; the gels were stained with Coomassie Brilliant Blue G-250 (panel A). Panels B and C show the progress of BMP1 cleavage of prodomains as assessed from the decrease of the amount of uncleaved prodomain (PD) and increase in the amount of C-terminal (PD_CT) and N-terminal (PD_NT) fragments resulting from BMP1-cleavage of the prodomain; the error bars indicate the standard error of the mean, $n = 3$. Note that in the absence of heparin, the D288A mutant WFIKKN1 had little effect on the cleavage of latent myostatin (panel B), whereas in the presence of heparin, the D288A mutant WFIKKN1 enhanced the cleavage of myostatin prodomain (panel C). Abbreviations: LM, latent myostatin; M, myostatin; PD, myostatin prodomain; PD_CT, C-terminal fragment of myostatin prodomain; PD_NT, N-terminal fragment of myosatin prodomain; W1_D288A, D288A mutant WFIKKN1.

TARNAAGLLRADFPLSVVQREPA**RD**AAPSIPAPAE) that connects the immunoglobulin and the first Kunitz domain of WFIKKN1. It is plausible to assume that the flexibility of this disordered linker region plays a key role in the susceptibility of this peptide bond to BMP1-cleavage. Although the low-resolution solution structure of WFIKKN1 [29] tells us very little about the position of the various regions in the globular-like structure of this multidomain protein, our data suggest that the linker region connecting the N-terminal and C-terminal halves of WFIKKN1 protein is exposed and accessible for BMP1.

Rate of cleavage of latent myostatin by BMP1 is not enhanced by the D288A mutant WFIKKN1 in the absence of heparin

To decide whether full-length WFIKKN1 has rate-enhancing activity, we substituted the Asp288 residue with alanine to render the protein resistant to BMP1-cleavage. As shown in Fig. 4 (panel B), when latent myostatin was digested with BMP1 in the absence of heparin, the rate of cleavage of myostatin prodomain was practically unaffected by increasing concentrations (0.5–4 µM) of D288A mutant WFIKKN1 protein,

Table 1. Comparison of the BMP1-cleavage site of WFIKKN with those of known substrates of BMP1.

Substrate	P4	P3	P2	P1	P1′	P2′	P3′	P4′
WFIKKN1	Glu	Pro	Ala	Arg	**Asp**	Ala	Ala	Pro
Alpha-2-macroglobulin	Phe	Tyr	Glu	Ser	**Asp**	Val	Met	Gly
Apolipoprotein A-I	Phe	Trp	Gln	Gln	**Asp**	Glu	Pro	**Pro**
Heparan sulfate proteoglycan	Ser	Gly	Gly	Asn	**Asp**	**Ala**	Pro	Gly
Biglycan	Leu	Met	Met	Asn	**Asp**	Glu	Glu	Ala
Chordin precursor	Arg	Ser	Tyr	Ser	**Asp**	Arg	Gly	Glu
Chordin precursor	Pro	Met	Gln	Ala	**Asp**	Gly	Pro	Arg
Collagen alpha 1(I) precursor	Tyr	Tyr	Arg	Ala	**Asp**	Asp	**Ala**	Asn
Collagen alpha 1(II) precursor	Tyr	Met	Arg	Ala	**Asp**	Glu	**Ala**	Ala
Collagen alpha 1(VII) precursor	Ser	Tyr	**Ala**	Ala	**Asp**	Thr	**Ala**	Gly
Collagen alpha 2(I) precursor	Phe	Tyr	Arg	Ala	**Asp**	Gln	Pro	Arg
Collagen alpha-1(I) chain	Tyr	Tyr	Arg	Ala	**Asp**	Asp	**Ala**	Asn
Collagen alpha-1(II) chain	Tyr	Met	Arg	Ala	**Asp**	Gln	**Ala**	Ala
Collagen alpha-1(III) chain	Pro	Tyr	Tyr	Gly	**Asp**	Glu	Pro	Met
Collagen alpha-1(V) chain	Thr	**Pro**	Gln	Ser	Gln	Asp	Pro	Asn
Collagen alpha-1(V) chain	Gln	Leu	Leu	Asp	**Asp**	Gly	Asn	Gly
Collagen alpha-1(XI) chain	Ala	Ala	Gln	Ala	Gln	Glu	Pro	Gln
Collagen alpha-2(V) chain	**Glu**	Phe	Thr	Glu	**Asp**	Gln	**Ala**	Ala
Collagen alpha-2(XI) chain	Arg	**Pro**	Gln	Asn	Gln	Gln	Pro	His
Collagen alpha-3(V) chain	Ser	Phe	Gln	Gln	Ala	Gln	**Ala**	Gln
Decorin precursor	Phe	Met	Leu	Glu	**Asp**	Glu	**Ala**	Ser
Dentin matrix acidic phosphoprotein 1	Gly	Met	Gln	Ser	**Asp**	Asp	Pro	Glu
DSPP600	Ser	Met	Gln	Gly	**Asp**	Asp	Pro	Asn
gldn gliomedin	Val	Ile	Pro	Asn	**Asp**	Asp	Thr	Leu
Growth/differentiation factor 11 precursor	Asp	Phe	Gln	Gly	**Asp**	**Ala**	Leu	Gln
Growth/differentiation factor 8 precursor	Asp	Val	Gln	**Arg**	**Asp**	Asp	Ser	Ser
Insulin-like growth factor-binding protein	**Glu**	Ser	Gln	Ser	Thr	Asp	Thr	Gln
Insulin-like growth factor-binding protein 3	Tyr	Glu	Ser	Gln	Ser	Thr	Asp	Thr
Laminin subunit gamma-2	Cys	Tyr	Ser	Gly	**Asp**	Glu	Asn	**Pro**
Latent-transforming growth factor beta-binding protein 1	Ile	**Pro**	Ser	Leu	**Asp**	Gln	Glu	Lys
Latent-transforming growth factor beta-binding protein 1	Tyr	Phe	Ile	Gln	**Asp**	Arg	Phe	Leu
Lysyl oxidase homolog 3	Leu	Ile	Cys	Gly	**Asp**	Asp	Trp	Gly
Lysyl oxidase-like 1	Val	Ala	Val	Gly	**Asp**	Ser	Thr	Gly
Lysyl oxidase-like 1	Val	Arg	Ser	Ser	**Asp**	**Ala**	Pro	**Pro**
Osteoglycin	Gln	Leu	Gln	Lys	**Asp**	Glu	Val	Ile
Probiglycan	Phe	Met	Met	Asn	**Asp**	Glu	Glu	Ala
Prolactin	Leu	Gln	Met	Ala	**Asp**	Glu	Glu	Ser
Prolysyl oxidase	Arg	Met	Val	Gly	**Asp**	Asp	Pro	Tyr
Prolysyl oxidase	Gly	Met	Val	Gly	**Asp**	Asp	Pro	Tyr
Prolysyl oxidase-like 1	Val	Ala	Val	Gly	**Asp**	Ser	Thr	Gly
Somatotropin	Asn	Ser	His	Asn	**Asp**	Asp	**Ala**	Leu

Information on known peptide substrates of BMP1 (peptidase M12.005: procollagen C-peptidase) was compiled from the MEROPS database; http://merops.sanger.ac.uk/cgi-bin/substrates?id=M12.005. Residues identical with those in the P4-P4′ positions of WFIKKN1's cleavage site are highlighted in bold.

suggesting that the marked rate enhancement observed in the case of the wild-type WFIKKN1 protein in the absence of heparin (see Fig. 3, panel B) is caused by the BMP1-cleavage product KKN1 and not the full-length protein. In harmony with this conclusion, when latent myostatin was digested with BMP1 in the absence of heparin, recombinant KKN1 protein (0.5–4 μM) significantly enhanced the rate of cleavage of myostatin prodomain (Fig. 5, panel B). The efficiency of KKN1 is illustrated by the fact that maximal enhancer activity was achieved even by 0.5 μM KKN1, the lowest concentration of KKN1 tested.

The most plausible explanation for the observation that WFIKKN1 is less active as an enhancer than the KKN1 fragment is that in the compact globular-like structure of WFIKKN1 [29], interdomain interactions render the NTR domain less accessible for interaction with the myostatin prodomain. According
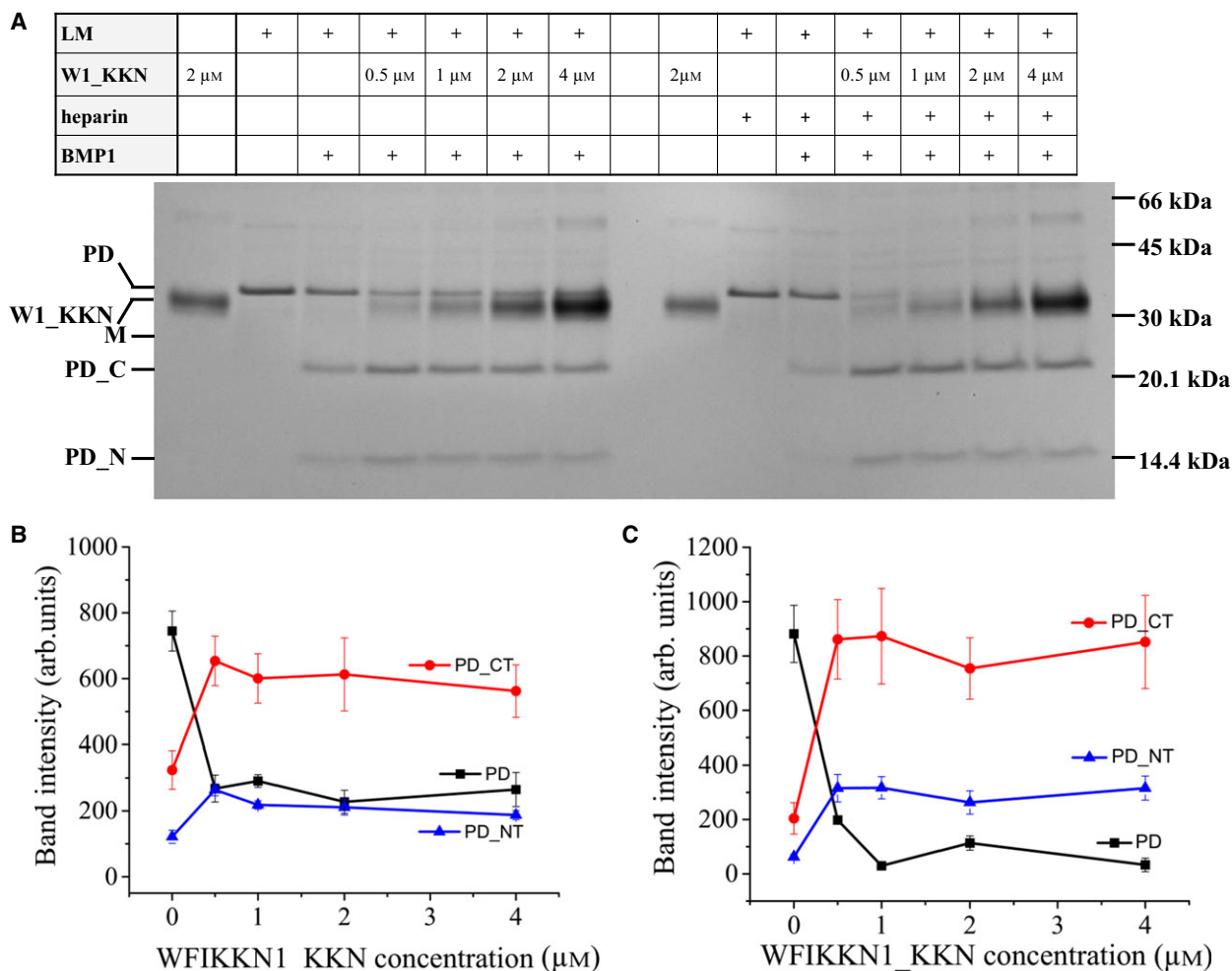
LM		+	+	+	+	+	+			+	+	+	+	+	+
W1_KKN	2 μM			0.5 μM	1 μM	2 μM	4 μM		2μM			0.5 μM	1 μM	2 μM	4 μM
heparin										+	+	+	+	+	+
BMP1			+	+	+	+	+				+	+	+	+	+

Fig. 5. Rate of cleavage of latent myostatin by BMP1 is significantly enhanced by KKN1. Latent human myostatin (LM, 500 nM) was digested with 50 nM BMP1 in 25 mM HEPES buffer, pH 7.5 containing 150 mM NaCl, 5 mM CaCl$_2$, 1 mM ZnCl$_2$, and 1 mM furin inhibitor I at 37 °C for 16 h in the presence of increasing concentrations of KKN1, in the absence or presence of heparin (5 μg·mL^{-1}). Nonreduced samples were analyzed by SDS/PAGE analysis; the gels were stained with Coomassie Brilliant Blue G-250 (panel A). Panels B and C show the progress of BMP1 cleavage of prodomains as assessed from the decrease of the amount of uncleaved prodomain (PD) and increase in the amount of C-terminal (PD_CT) and N-terminal (PD_NT) fragments resulting from BMP1-cleavage of the prodomain; the error bars indicate the standard error of the mean, $n = 3$. Note that KKN1 enhanced the cleavage of latent myostatin both in the absence (panel B) and presence of heparin (panel C). Abbreviations: LM, latent myostatin; M, myostatin; PD, myostatin prodomain; PD_CT, C-terminal fragment of myostatin prodomain; PD_NT, N-terminal fragment of myosatin prodomain; W1_KKN, the KKN fragment of WFIKKN1.

to this explanation, cleavage of WFIKKN1 by BMP1 liberates the KKN1 fragment from these interactions, thereby increasing the accessibility of the NTR domain and favoring its interaction with myostatin prodomain.

It should be noted, however, that in the presence of heparin, the D288A mutant WFIKKN1 protein also has detectable enhancer activity (Fig. 4, panel C). Similarly, the enhancer activity of KKN1 was more pronounced when heparin was included in the reaction mixture (compare panels B and C of Fig. 5).

Molecular basis of the enhancer activity of KKN1 on BMP1 activation of latent myostatin

To get an insight into the molecular basis of the enhancer activity of KKN1 on BMP1-cleavage of latent myostatin we have analyzed the structural characteristics of the BMP1-cleavage sites of homodimeric latent myostatin [11].

In the homology model of homodimeric latent myostatin (based on the crystal structure of homodimeric pro-TGF-β1 [30]), the two monomers form a disk-like

circular structure (Fig. 6). N-terminal parts of the two prodomains, consisting of the α1 and α2 helices, provide the 'straitjacket' that encircles and shields each growth factor monomer of the homodimer, whereas the C-terminal parts of the two prodomains provide the 'arm domains' that connect the two prodomains in the homodimeric precursor. The 'arm domains' consist of three distinct structural regions. A four-stranded β-sheet (consisting of β1, β3, β6, and β10 strands and buried by the α2, α3, and α4 helices) is in close proximity of the growth factor monomer of the same polypeptide chain, whereas a four-stranded β-sheet (consisting of β2, β4, β5, and β7 strands) and β-strands β8 and β9 extend to link the two arm domains of the homodimeric precursor in a 'bowtie'.

The loops containing the BMP1-cleavage sites of latent myostatin are buried in the center of the disk-like homodimer (Fig. 6), suggesting that they are not readily accessible to cleavage by BMP1. The most plausible explanation for the enhancer activity of KKN1 is that binding of the NTR domain of KKN1 to the C-terminal subdomains of myostatin prodomains [18,26] loosens the 'bowtie', shifting the conformational equilibrium from the circular structure toward a more open form of latent myostatin making the BMP1-cleavage sites more accessible to the enzyme.

Heparin-dependence of the activity of WFIKKN1 proteins as enhancers of BMP1-mediated activation of latent myostatin

The heparin-dependence of the BMP1-enhancer activity of WFIKKN1 (Fig. 3), D288A mutant WFIKKN1 (Fig. 4) and KKN1 (Fig. 5), is reminiscent of the heparin-dependence of the BMP1-enhancer activity of procollagen C-proteinase enhancer-1 protein (PCPE-1). According to the model proposed by Bekhouche *et al.* [31], the enhancer PCPE-1 binds to the substrate procollagen III C-propeptides with high affinity and this PCPE-1/procollagen complex binds to heparin-like glycosaminoglycans via the NTR domain of PCPE-1 as well as via procollagen III. As BMP1 also interacts with heparin, these interactions increase the local concentrations of the reactants facilitating the action of BMP1 [31].

We assume that an analogous model might explain the heparin-dependence of the BMP1-enhancer activity of WFIKKN1_D288A and KKN1 proteins, with latent myostatin as substrate. A key aspect of this model is that BMP1, latent myostatin, and WFIKKN1 proteins are all bound to heparin and the increased local concentration of the reactants facilitates the action of BMP1 on latent myostatin. It is well established that latent myostatin [12] and BMP1 [32] have affinity for heparin,
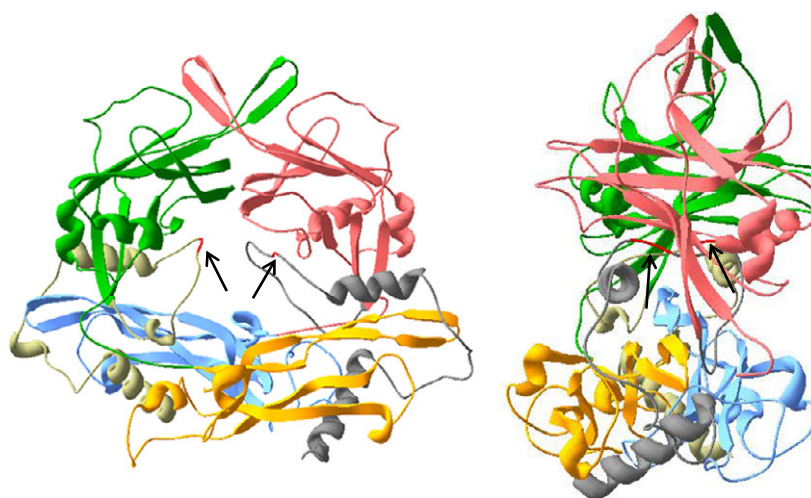

Fig. 6. The BMP1-cleavage sites are buried in the center of the homodimer of latent myostatin. In the homology model of homodimeric latent myostatin, the two monomers form a disk-like circular structure. N-terminal parts of the two prodomains (pale yellow – light gray) provide the 'straitjacket' that encircles and shields each growth factor monomer of the homodimer (light blue – yellow), whereas the C-terminal parts of the two prodomains (green – pink) provide the 'arm domains' that connect the two prodomains in the homodimeric precursor in a 'bowtie'. The loops containing the BMP1-cleavage sites of latent myostatin are buried in the center of the disk-like homodimer, suggesting that they are not readily accessible to cleavage by BMP1. Our data suggest that binding of the NTR domain of KKN1 to the C-terminal subdomains of myostatin prodomains loosens the 'bowtie', shifting the conformational equilibrium from the circular structure to a more open form of latent myostatin making the BMP1 cleavage sites more accessible to the enzyme. The black arrows indicate the position of the BMP1 cleavage sites between residues Arg98–Asp99. The positions of Arg98 and Asp99 are highlighted in red. The figure in the right-hand panel was generated by 90° clockwise rotation of the homodimer around the *y*-axis.

and in the present work, we have found evidence that WFIKKN1 proteins also have significant affinity for heparin. As shown in Fig. 7, both WFIKKN1 and KKN1 have affinity for immobilized heparin. Interestingly, KKN1 has higher affinity for heparin than the full-length protein, suggesting that intramolecular interactions of the compact globular WFIKKN1 protein may partially bury the heparin-binding site. In view of these findings, it seems likely that BMP1-cleavage of WFIKKN1 favors the formation of the enhancer complex, not only by increasing the accessibility of the NTR domain for the myostatin prodomain but also by increasing the heparin affinity of the enhancer.

In summary, in the present work we have shown that WFIKKN1 is cleaved by BMP1 generating the C-terminal KKN1 fragment that is a potent heparin-dependent enhancer of BMP1-activation of latent myostatin. BMP1-cleavage of WFIKKN1 protein and latent myostatin are thus synergistic in the sense that they promote the liberation of active myostatin from latent myostatin complex.

Materials and methods

Reagents, enzymes, PCR primers, proteins, bacterial strains

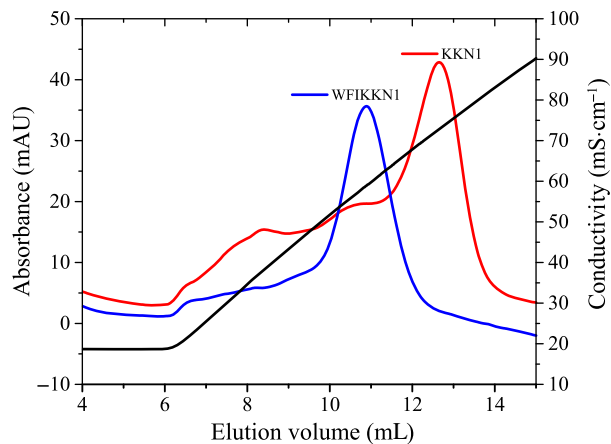Mutagenesis primers were from Integrated DNA Technologies (Coralville, IA, USA). The mutagenesis reaction was

Fig. 7. The WFIKKN1 and KKN1 proteins have affinity for heparin. About 1 mL aliquots of WFIKKN1 (5 μM) or KKN1 (5 μM) dissolved in 50 mM Tris/HCl, 150 mM NaCl buffer, pH 7.5 were applied on 1 mL Hitrap Heparin Sepharose columns. The columns were washed with 5 mL of buffer containing 50 mM Tris/HCl, 150 mM NaCl, pH 7.5 and the proteins were eluted with a 10 mL gradient of buffer A (50 mM Tris/HCl, 150 mM NaCl, pH 7.5) and buffer B (50 mM Tris/HCl, 1.5 M NaCl, pH 7.4). Note that isolated KKN1 has higher affinity for heparin than full-length WFIKKN1.

performed with Quickchange mutagenesis kit (Agilent Technologies, Inc. Santa Clara, CA USA). DNA was purified with Nucleospin Extract DNA purification kit (Macherey-Nagel, Duren, Germany). *Escherichia coli* JM109 was used for DNA propagation during DNA manipulation steps, and *E. coli* BL21(DE3) strain was used for protein expression.

Recombinant human promyostatin, human WFIKKN1, and human WFIKKN2 were produced as described previously [18,19,26].

Recombinant furin, recombinant BMP1, (R&D Systems, Minneapolis, MN, USA), furin inhibitor I (Merck Millipore, Darmstadt, Germany), and heparin (Sigma-Aldrich, St Louis, MO, USA) were commercial products. HiTrap Heparin HP columns were obtained from GE Healthcare Life Sciences (Budapest, Hungary).

FUGENE HD transfection reagent was purchased from Promega (Madison, WI, USA). The culture media and fetal bovine serum used for Drosophila S2 cell maintenance, selection, and protein expression were from Invitrogen/ThermoFisher Scientific (Waltham, MA, USA).

Production of the D288A mutant of human WFIKKN1 in *Drosophila melanogaster S2* cells

Mutagenesis was performed with QuikChange Site-Directed Mutagenesis method with the 5′CGAGAGCCGGCCAG GGCCGCAGCCCCCAGCATCC3′ sense and 5′GGATG CTGGGGGGCTGCGGCCCTGGCCGGCTCTCG 3′anti-sense primers. The *Drosophila* expression vector pMT/BiP/V5/His A containing the cDNA of human WFIKKN1 protein [18] was the template in the mutagenesis reaction. The mutagenesis introduced an A to C change at position 863 of the human WFIKKN1 cDNA causing the D288A mutation in the protein. The presence of the mutation was confirmed by DNA sequencing and the plasmid pMT/BiP/WFIKKN1_D288A was used to produce stable transfected *Drosophila melanogaster S2* cells.

Drosophila melanogaster S2 cells (Drosophila Genomics Resource Center, Indiana University, Bloomington, IN, USA) were transformed in Schneider Drosophila Medium containing 10% heat inactivated fetal bovine serum. The expression plasmid pMT/BiP/WFIKKN1_D288A and pCo-Hygro selection vector were mixed in a 19 : 1 ratio and 5 μg of the mixture was dissolved in 250 μL OPTIMEM medium then 15 μL FUGENE HD transfection reagent was added. Complex formation was allowed for 10 min then the plasmid solution was added to 1×10^6 *D. melanogaster S2* cells in 5 mL medium. About 24 h later, the media containing the transfection mixture was removed and the cells were suspended in 5 mL of fresh Schneider Drosophila Medium supplemented with 10% fetal bovine serum. Selection of stable transfectants was initiated 96 h post transfection by the addition of 300 μg·mL^{-1} hygromycin B to the culture medium. The cells were grown for 72 h and the medium was replaced by 5 mL of medium containing 70% of fresh

Schneider *Drosophila* Medium and 30% of conditioned medium collected from growing S2 cells and 300 µg·mL^{-1} hygromycin B was added. These steps were repeated every third day and stably transformed polyclonal lines were established after 5 weeks of selection.

Expression and purification of recombinant proteins secreted by S2 cells was performed essentially as described previously [18]. Stable transfectants were grown in Express five serum-free insect medium to a cell density of 2–3 × 10^6 per mL, and protein expression was induced by adding CuSO$_4$ at 300 µM final concentration. After 1 week of induction, the culture was centrifuged and the medium was dialyzed against 50 mM Tris/HCl buffer, pH 7.5, and applied onto a Ni-NTA Sepharose column. The column was washed with 10 column volumes of 20 mM Tris/HCl buffer, pH 7.9, containing 500 mM NaCl and 5 mM imidazole then with 5 column volumes of 20 mM Tris/HCl buffer, pH 7.9, containing 500 mM NaCl and 30 mM imidazole, and the bound protein was eluted with 20 mM Tris/HCl buffer, pH 7.9 containing 300 mM imidazole. The eluted protein was concentrated on Amicon Ultra-15 centrifugal filter devices and chromatographed on a Superdex 300 column equilibrated with 100 mM ammonium bicarbonate buffer, pH 8.0.

Production of the KKN1 fragment of WFIKKN1 protein in *Drosophila melanogaster*

The cDNA coding for fragments of WFIKKN1 protein were amplified with Phusion high fidelity polymerase (New England Biolabs, Ipswich, MA, USA) using the plasmid containing the full-length WFIKKN1 cDNA as template. The cDNA of the fragment containing the two Kunitz domains and the NTR domain (KKN1) was amplified with 5′GG AAGATCTGACGCAGCCCCCAGCATCCCA3′ sense and 5′GGAACCGGTGTCCTGGAAGCGGTTGAGCAGC3′ antisense primers. The amplimers were digested with BglII and AgeI enzymes and ligated into pMT/BiP/V5/HisA expression plasmid digested with the same enzymes. *Drosophila melanogaster* S2 cells were transfected with the plasmid pMT/BiP/KKN1 using the protocol described in section 4.2 and KKN1 protein was purified from the media as described above.

Proteolytic digestion of promyostatin with furin in the presence and absence of WFIKKN proteins

To monitor the influence of WFIKKN1 (1.5 µM) and WFIKKN2 (1.5 µM) on furin-mediated cleavage of promyostatin, human promyostatin (0.5 µM) was digested with human furin (1 µg·mL^{-1}) in 100 mM Tris/HCl, 150 mM NaCl, 1 mM CaCl$_2$, 100 µM PMSF buffer, pH 8.0 at 28 °C. Aliquots were removed at various time points (0, 5, 15, 30 min, 1, 4, 24 h) and the composition of the samples was analyzed by SDS/PAGE.

Proteolytic digestion of latent myostatin with human BMP1 in the presence and absence of WFIKKN1 protein

Latent myostatin was produced by digesting promyostatin (1 µM) with 3.5 µg·mL^{-1} furin in 100 mM Tris/HCl, 150 mM NaCl, 1 mM CaCl$_2$, 100 µM PMSF buffer, pH 8.0 at 28 °C for 24 h. The digestion was arrested with 1 µM furin inhibitor I; samples were stored at −20 °C.

To monitor the influence of WFIKKN1 protein (0.5, 1, 2, 4 µM) on BMP1-cleavage of latent myostatin by SDS/PAGE, latent myostatin (0.5 µM) was digested with BMP1 (50 nM) in 25 mM HEPES buffer, pH 7.5 containing 150 mM NaCl, 5 mM CaCl$_2$, 1 µM ZnCl$_2$, and 1 µM furin inhibitor I at 37 °C for 16 h and the composition of the samples was analyzed by SDS/PAGE. The experiments were also performed in the presence of 5 µg·mL^{-1} heparin.

Protein analyses

The concentrations of the recombinant proteins were determined using the following extinction coefficients: promyostatin monomer, 55 640 M^{-1}·cm^{-1}; WFIKKN1, 64 440 M^{-1}·cm^{-1}; WFIKKN2, 57 470 M^{-1}·cm^{-1}; KKN1, 32 065 M^{-1}·cm^{-1}; the extinction coefficients were calculated with the online protein analysis tool PROTPARAM. (http://web.expasy.org/protparam/).

The composition of protein samples was analyzed by SDS/PAGE under both reducing and nonreducing conditions; unless otherwise indicated, the gels were stained with Coomassie Brilliant Blue G-250. For quantitative evaluation of protein compositions, the stained gels were scanned with the ChemiImager 5500 gel documentation instrument (Alpha Innotech, San Leandro, CA, USA) and the intensities of the protein bands were quantified with GELQUANT.NET software of BiochemLabSolutions (University of California, San Francisco UCSF). In the case of each electropherogram, quantitative evaluation of protein composition was repeated six times.

To compare the rates of furin-mediated cleavage of promyostatin in the presence and absence of WFIKKN proteins, we monitored the changes in the band intensity of myostatin prodomain formed as a result of furin-cleavage. The rates of BMP1-mediated cleavage of latent myostatin in the presence and absence of WFIKKN proteins were compared in a similar way except that in this case we monitored the changes in the band intensities of uncleaved myostatin prodomain as well as the two fragments generated by BMP1-cleavage of the prodomain. All experiments were performed in triplicate.

N-terminal sequencing of proteins was performed on an Applied Biosystems 471A protein sequencer with an online ABI 120A phenylthiohydantoin (PTH) analyzer.

Hitrap Heparin Sepharose chromatography

One milliliter aliquots of WFIKKN1 (5 μM) or KKN1 (5 μM) in 50 mM Tris/HCl, 150 mM NaCl buffer, pH 7.5 were applied on 1 mL Hitrap Heparin Sepharose columns. The columns were washed with 5 mL of buffer containing 50 mM Tris/HCl, 150 mM NaCl, pH 7.5, and the proteins were eluted with a 10 mL gradient of buffer A (50 mM Tris/HCl, 150 mM NaCl, pH 7.5) and buffer B (50 mM Tris/HCl, 1.5 M NaCl, pH 7.4).

Protein modeling

The homology model of promyostatin was generated with the automated protein structure homology-modeling server SWISS-MODEL Version 8.05 (http://swissmodel.expasy.org) as described previously [11].

Acknowledgements

Author contributions

MT and LP conceived and designed the experiments. GS, VV, and MT performed the experiments. GS, VV, MT, and LP analyzed the data. LP wrote the paper.

References

1 McPherron AC, Lawler AM & Lee SJ (1997) Regulation of skeletal muscle mass in mice by a new TGF-beta superfamily member. *Nature* **387**, 83–90.

2 Szabó G, Dallmann G, Müller G, Patthy L, Soller M & Varga L (1998) A deletion in the myostatin gene causes the compact (Cmpt) hypermuscular mutation in mice. *Mamm Genome* **9**, 671–672.

3 Grobet L, Martin LJ, Poncelet D, Pirottin D, Brouwers B, Riquet J, Schoeberlein A, Dunner S, Menissier F, Massabanda J *et al.* (1997) A deletion in the bovine myostatin gene causes the double-muscled phenotype in cattle. *Nat Genet* **17**, 71–74.

4 Kambadur R, Sharma M, Smith TP & Bass JJ (1997) Mutations in myostatin (GDF8) in double-muscled Belgian Blue and Piedmontese cattle. *Genome Res* **7**, 910–916.

5 McPherron AC & Lee SJ (1997) Double muscling in cattle due to mutations in the myostatin gene. *Proc Natl Acad Sci USA* **94**, 12457–12461.

6 Mosher DS, Quignon P, Bustamante CD, Sutter NB, Mellersh CS, Parker HG & Ostrander EA (2007) A mutation in the myostatin gene increases muscle mass and enhances racing performance in heterozygote dogs. *PLoS Genet* **3** (5), e79.

7 Schuelke M, Wagner KR, Stolz LE, Hubner C, Riebel T, Kömen W, Braun T, Tobin JF & Lee SJ (2004) Myostatin mutation associated with gross muscle hypertrophy in a child. *N Engl J Med* **350**, 2682–2688.

8 McPherron AC & Lee SJ (2002) Suppression of body fat accumulation in myostatin-deficient mice. *J Clin Invest* **109**, 595–601.

9 Lin J, Arnold HB, Della-Fera MA, Azain MJ, Hartzell DL & Baile CA (2002) Myostatin knockout in mice increases myogenesis and decreases adipogenesis. *Biochem Biophys Res Commun* **291**, 701–706.

10 Anderson SB, Goldberg AL & Whitman M (2008) Identification of a novel pool of extracellular pro-myostatin in skeletal muscle. *J Biol Chem* **283**, 7027–7035.

11 Szláma G, Trexler M, Buday L & Patthy L (2015) K153R polymorphism in myostatin gene increases the rate of promyostatin activation by furin. *FEBS Lett* **589**, 295–301.

12 Lee SJ & McPherron AC (2001) Regulation of myostatin activity and muscle growth. *Proc Natl Acad Sci USA* **98**, 9306–9311.

13 Thies RS, Chen T, Davies MV, Tomkinson KN, Pearson AA, Shakey QA & Wolfman NM (2001) GDF-8 propeptide binds to GDF-8 and antagonizes biological activity by inhibiting GDF-8 receptor binding. *Growth Factors* **18**, 251–259.

14 Wolfman NM, McPherron AC, Pappano WN, Davies MV, Song K, Tomkinson KN, Wright J, Zhao L, Sebald SM, Greenspan DS *et al.* (2003) Activation of latent myostatin by the BMP-1/tolloid family of metalloproteinases. *Proc Natl Acad Sci USA* **100**, 15842–15846.

15 Lee SJ (2008) Genetic analysis of the role of proteolysis in the activation of latent myostatin. *PLoS One* **3**, e1628.

16 Hill JJ, Davies MV, Pearson AA, Wang JH, Hewick RM, Wolfman NM & Qiu Y (2002) The myostatin propeptide and the follistatin-related gene are inhibitory binding proteins of myostatin in normal serum. *J Biol Chem* **277**, 40735–40741.

17 Hill JJ, Qiu Y, Hewick RM & Wolfman NM (2003) Regulation of myostatin in vivo by growth and differentiation factor-associated serum protein-1: a novel protein with protease inhibitor and follistatin domains. *Mol Endocrinol* **17**, 1144–1154.

18 Kondás K, Szláma G, Trexler M & Patthy L (2008) Both WFIKKN1 and WFIKKN2 have high affinity for growth and differentiation factors 8 and 11. *J Biol Chem* **283**, 23677–23684.

19 Szláma G, Kondás K, Trexler M & Patthy L (2010) WFIKKN1 and WFIKKN2 bind growth factors TGFβ1, BMP2 and BMP4 but do not inhibit their signalling activity. *FEBS J* **277**, 5040–5050.

20 Haidet AM, Rizo L, Handy C, Umapathi P, Eagle A, Shilling C, Boue D, Martin PT, Sahenk Z, Mendell JR *et al.* (2008) Long-term enhancement of skeletal muscle mass and strength by single gene administration of myostatin inhibitors. *Proc Natl Acad Sci USA* **105**, 4318–4322.

21 Monestier O, Brun C, Heu K, Passet B, Malhouroux M, Magnol L, Vilotte JL & Blanquet V (2012) Ubiquitous Gasp1 overexpression in mice leads mainly to a hypermuscular phenotype. *BMC Genom* **13**, 541.

22 Trexler M, Bányai L & Patthy L (2001) A human protein containing multiple types of protease-inhibitory modules. *Proc Natl Acad Sci USA* **98**, 3705–3709.

23 Trexler M, Bányai L & Patthy L (2002) Distinct expression pattern of two related human proteins containing multiple types of protease-inhibitory modules. *Biol Chem* **383**, 223–228.

24 Kondás K, Szláma G, Nagy A, Trexler M & Patthy L (2011) Biological functions of the WAP domain-containing multidomain proteins WFIKKN1 and WFIKKN2. *Biochem Soc Trans* **201139**, 1416–1420.

25 Nagy A, Trexler M & Patthy L (2003) Expression, purification and characterization of the second Kunitz-type protease inhibitor domain of the human WFIKKN protein. *Eur J Biochem* **270**, 2101–2107.

26 Szláma G, Trexler M & Patthy L (2013) Latent myostatin has significant activity and this activity is controlled more efficiently by WFIKKN1 than by WFIKKN2. *FEBS J* **280**, 3822–3839.

27 Mac Sweeney A, Gil-Parrado S, Vinzenz D, Bernardi A, Hein A, Bodendorf U, Erbel P, Logel C & Gerhartz B (2008) Structural basis for the substrate specificity of bone morphogenetic protein 1/tolloid-like metalloproteases. *J Mol Biol* **384**, 228–239.

28 Hopkins DR, Keles S & Greenspan DS (2007) The bone morphogenetic protein 1/Tolloid-like metalloproteinases. *Matrix Biol* **26**, 508–523.

29 Walker RG, Angerman EB, Kattamuri C, Lee YS, Lee SJ & Thompson TB (2015) Alternative binding modes identified for growth and differentiation factor-associated serum protein (GASP) family antagonism of myostatin. *J Biol Chem* **290**, 7506–7516.

30 Shi M, Zhu J, Wang R, Chen X, Mi L, Walz T & Springer TA (2011) Latent TGF-β structure and activation. *Nature* **474**, 343–349.

31 Bekhouche M, Kronenberg D, Vadon-Le Goff S, Bijakowski C, Lim NH, Font B, Kessler E, Colige A, Nagase H, Murphy G *et al.* (2010) Role of the netrin-like domain of procollagen C-proteinase enhancer-1 in the control of metalloproteinase activity. *J Biol Chem* **285**, 15950–15959.

32 Wozney JM, Rosen V, Celeste AJ, Mitsock LM, Whitters MJ, Kriz RW, Hewick RM & Wang EA (1988) Novel regulators of bone formation: molecular clones and activities. *Science* **242**, 1528–1534.